

A Study on the Wide-Sense Stationarity of the Underwater Acoustic Channel for Non-coherent Communication Systems

(Invited Paper)

Beatrice Tomasi*, James Preisig[†], Grant B. Deane[‡], and Michele Zorzi*

*Department of Information Engineering — University of Padova, Italy

[†]Department of Applied Ocean Physics and Engineering — Woods Hole Oceanographic Institution, (MA) USA

[‡]Marine Physical Laboratory — Scripps Institution of Oceanography, La Jolla, (CA) USA

Email: tomasibe@dei.unipd.it, jpreisig@whoi.edu, gdeane@ucsd.edu, zorzi@dei.unipd.it

Abstract—In this paper we study the wide sense stationarity of the energy of the underwater acoustic channel impulse response and we provide an estimate of the interval during which the wide sense stationarity property holds. We analyze the SPACE08 data set, which has been collected near Martha’s Vineyard Island during October 2008. In this data set the environmental conditions such as the height of the waves and the wind direction vary significantly in time. We consider the time series recorded in four different fixed positions. This allows us to compare the results between different locations and environmental conditions.

I. INTRODUCTION

The improvement of the performance of underwater acoustic communications systems has been an active area of research for a number of years. One avenue of work has focused on optimizing system parameters (e.g., transmit power, symbol rate, error correction coding rate) to maximize the channel throughput given limited resources. In order to more efficiently use the channel, a data adaptive estimator, able to predict the quality¹ of the channel, could be applied. However these estimators are optimized for estimates of channel statistics, hence they assume that the channel fluctuations (of its energy in our case) can be represented as a wide sense stationary (WSS) random process. It is therefore important to understand the time interval over which the channel energy evolution can be modeled as a WSS random process.

For these reasons, in this paper we test the wide sense stationarity of the channel energy and we estimate the interval over which the channel can be modeled as WSS. We choose the total energy in the channel impulse response because it is a metric of the quality of the received signal, especially for non-coherent receivers, e.g., as used in M-ary Frequency Shift Keying (MFSK) or Frequency Hopping MFSK modulation systems, which are often implemented in underwater acoustic modems (for example these modulation schemes are supported by [1] and [2]). In this paper, we use the methodology proposed in [3] which uses surrogates and a time-frequency

approach to test the stationarity of the channel. In this method, no assumption is made on the model which generates the data, and the test is based on the comparison of time-frequency features between a stationarized version of the data and the original data set.

Many stationarity tests have been extensively studied in the literature (such as those in [4], [5], [6]) and they have been applied in different disciplines (such as biology, neuroscience, signal processing, economics) but there are only few papers on the stationarity test for the wireless channel quality. In particular, these papers focus on the RF wireless channel, while the stationarity properties of the underwater acoustic channel have not been studied yet and this work is a first contribution to investigate this problem. Examples of RF-related stationarity studies include the following. In [7] the stationarity of the complex baseband channel for a radio mobile MIMO communication system is studied. In [8] the authors study another stationarity test for the MIMO channel and apply it to measured data, concluding that the greater the number of transmitters and receivers the shorter the stationarity interval of the MIMO channel. In [9] a study of the wide sense stationarity has been conducted on the multipath pattern for a car-to-car MIMO communication system.

In this work we analyze acoustic and environmental data collected during the Surface Processes and Acoustic Communications Experiment (SPACE08), and we evaluate the channel stationarity using signals transmitted from and received at fixed platforms. In contrast to common radio wireless scenarios, the communications channel exhibits time varying and statistically non-stationary behavior even without platform motion. In this case, due to the shallow water depth (approximately 15 meters), the scattering of the acoustic signals off surface waves affects a significant portion of the overall channel impulse response. The time-varying scattering off the surface waves results in a time-varying communications channel and environmental changes which change the characteristics of the surface wave field result in statistically non-stationary behavior of the fluctuations in the communications channel over time scales corresponding to the time scales of the environmental changes. After estimating the interval over which the channel

¹In this paper we consider the total energy in the channel impulse response (which is proportional to the signal to noise ratio) as a measure of the channel quality.



Fig. 1. A scheme of the testbed deployment off the coast of the Martha's Vineyard Island.

fluctuations can be treated as stationary, we estimate the power spectral density of the channel fluctuations over the interval of stationarity. We find a dependence of the power spectral density of the communications channel fluctuations particularly on the intensity of the wind driven surface wave variability.

The experiment was conducted during the month of October 2008 at the Martha's Vineyard Coastal Observatory (MVCO) operated by the Woods Hole Oceanographic Institution [10]. The data set is particularly interesting because the environmental conditions such as the surface wave characteristics and wind speed and direction varied significantly over the duration of the experiment. While the collected data sets are from only one deployment, the impact of surface variability on acoustic channel stationarity is more generally interpretable in other scenarios with similar geometries.

II. THE EXPERIMENTAL SCENARIO AND THE DATA SET

In this section we describe the scenario of the sea trials and the collected data set. We also show the time series of the estimated energy of the underwater acoustic channel, which we will use in the test of stationarity.

A. Scenario

The SPACE08 scenario consists of one transmitter and six fixed receiving stations, each of which is equipped with several hydrophones. Figure 1 represents the experimental setup: the four receiving stations that we will consider here are labeled as S3, S4, S5 and S6. In this work, we consider the data collected by one hydrophone at each of these systems. Systems S3 and S4 are 200 meters from the transmitter in the Southeast and Southwest directions, respectively. S5 and S6 are 1000 meters from the transmitter in the Southeast and Southwest directions, respectively. The seafloor at the experiment site was relatively flat.

In this paper we show the results of the analysis of data recorded from October 18 to October 27. The wind and wave conditions, shown in Figures 2 and 3, varied substantially over this period. For reference, Julian Date 292 was October 18 in 2008.

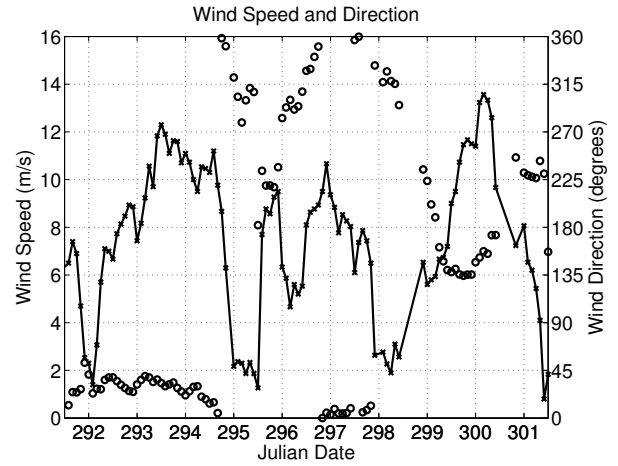


Fig. 2. Time series of the wind speed and direction. The solid line shows wind speed while the circles show wind direction.

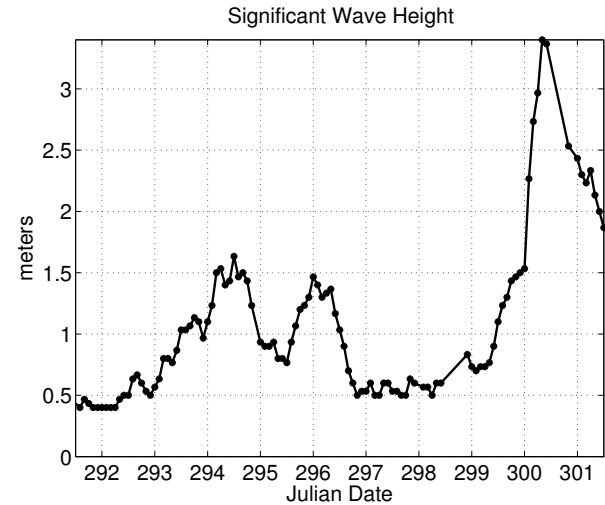


Fig. 3. Time series of the significant wave height. The significant wave height is defined as the average wave height of the one-third largest waves.

The transmitted signals consist of multiple repetitions of a 4095 point binary maximum length sequence transmitted at a symbol rate of 6.5 kbps and modulated at a central frequency of 11.5 kHz. A transmission three minutes in duration was made once every two hours. A maximum length sequence is a particular pseudo noise signal that is spectrally flat. Thanks to this property, it is possible to estimate the channel impulse response by computing the correlation between the transmitted signal and the received signal. We compute the channel estimate over segments of the received signal that are 400 symbols long (which corresponds to 60 ms). After each estimation we shift the window by 100 symbols, which corresponds to 15 ms, resulting in an estimate every 15 ms over windows of 60 ms.

B. The Channel Energy Time Series

In this subsection, we analyze the energy of the estimated channel impulse response, and its fluctuations in time. Calling

$g(t)$ the estimated channel impulse response measured in the time interval $t \in [0, NT_s]$, we estimate the energy as:

$$E_g = T_s \sum_{i=0}^{N-1} |g(i)|^2 \quad (1)$$

where T_s is the sampling interval. Figures 4(a), 4(b), 5(a) and 5(b) show the energy time series during Julian dates from 292 to 301 (which corresponds to days from October 18 to 27) in a dB scale. We can notice that the energy of the communication channel between the transmitter and the closest receivers (S3 and S4) is spread in the same interval, $[-26, -38]$ dB, while the energy of links between the source and systems S5 and S6 exhibits greater macro variability². More specifically the energy of the channel between the transmitter and S5 is in the interval $[-75, -45]$ dB, and the range of fluctuations at S5 is much greater than it is at S6. This observation implies that not only the distance but also the orientation between the transmitter and the receiver matter for underwater acoustic communications. It can be noticed that the four time series have the same main fluctuations: this suggests that those macro variabilities are due to environmental changes (such as the surface roughness) which affect the receivers in the same way. We observe a significant drop of the energy of the channel at receivers S5 and S6, around the Julian date 300: this can be explained by observing the environmental conditions during that period. In Figures 2 and 3, we observe high wind speed and large waves around date 300. These conditions are more likely to increase the surface wave breaking and the presence of significant subsurface bubbles. This can result in a larger attenuation and scattering of propagating acoustic signals that reflect off the surface as studied and reported in [11]. This effect is more evident for longer links.

III. RESULTS

In this section we describe the stationarity test and we show the estimated interval of stationarity for the data set described so far. A stochastic process is said to be WSS when its statistical moments of the first and second order are time invariant. In practice, when the stationarity property is to be tested for a time series, we could observe the fluctuations of the power spectral density (PSD). Estimating either the PSD or the correlation function requires the assumption that the data are stationary. We choose the framework proposed in [3], because no assumption is made on the model which generates the data, and the test is based on the comparison of time-frequency features between a stationarized version of the data and the original data set. After having run the stationarity test, we estimate the PSD of the energy over the stationarity interval. We will show the results and provide a physical explanation of these results by comparing the environmental and acoustical data.

²For macro variability we mean fluctuations over intervals of several hours

A. The Stationarity Test

In this section we summarize the procedure that we used, which is described in [3] (for more detail we refer the reader to that paper). The method aims at determining the stationarity time scale of a signal by comparing the local spectra statistics to the global spectrum, obtained by marginalization. We compute the local spectra by using the multitaper spectrogram defined as:

$$S_{g,K}(t, f) = \frac{1}{K} \sum_{k=1}^K S_g^{(h_k)}(t, f), \quad (2)$$

where $S_g^{(h_k)}(t, f)$ is the spectrogram computed with the k -th Hermite function, and is given by:

$$S_g^{(h_k)}(t, f) = \left| \int g(s) h_k(s-t) e^{-i2\pi f s} ds \right|^2. \quad (3)$$

The symbol $h_k(t)$ stands for the k -th Hermite function, whose length is T_h . We will vary T_h in order to test the stationarity for different time intervals. Usually what one can do is to consider the variability of the local spectra with respect to the global spectrum but, given that a variability is always observed, we need to compare these variations to those between the local and global spectra of the surrogate data. A surrogate data set is a stationarized version of the experimental data set. It is obtained by multiplying the amplitude of the Fourier transform of the original time series by an independent identically distributed phase sequence and then applying the inverse Fourier transform. In this way the correlation function of the obtained process depends only on the interval between two sequences and not on the absolute times at which they are taken. What we compute are just realizations of the random process, therefore computing more realizations by randomization improves the test. We will call the number of randomizations J . Then we compute the distance between the local spectra and the global spectrum (GS) obtained by marginalization, which can be expressed as:

$$GS = E[S_{g,K}(t, f)]_t = \frac{1}{T} \sum_{i=1}^T S_{g,K}(i, f). \quad (4)$$

The distance we compute is defined as a combination of the Kullback-Leibler divergence and the log-spectral deviation, respectively defined as [12]:

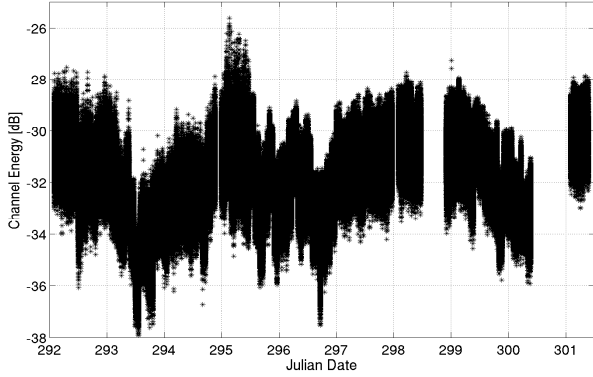
$$D_{KL}(L, G) = \int_{\Omega} (L(f) - G(f)) \log \frac{L(f)}{G(f)} df, \quad (5)$$

$$D_{LSD}(L, G) = \int_{\Omega} \left| \log \frac{L(f)}{G(f)} \right| df, \quad (6)$$

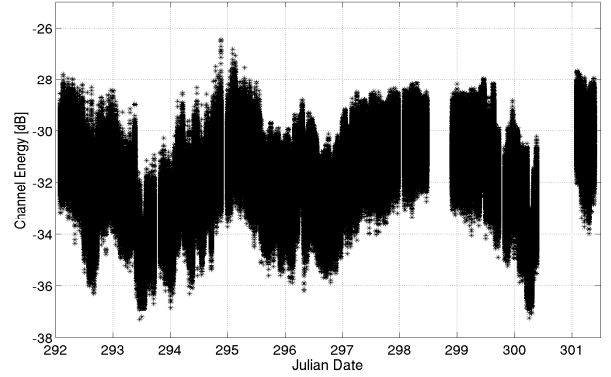
where $L(f)$ and $G(f)$ are respectively the local and the global spectrum, and f is the frequency variable over the space Ω . The combination that we consider is the following:

$$D(L, G) = D_{KL}(\tilde{L}, \tilde{G}) \cdot (1 + D_{LSD}(L, G)) \quad (7)$$

where \tilde{L} and \tilde{G} are the normalized versions of L and G . We compute the N distances between the N local spectra

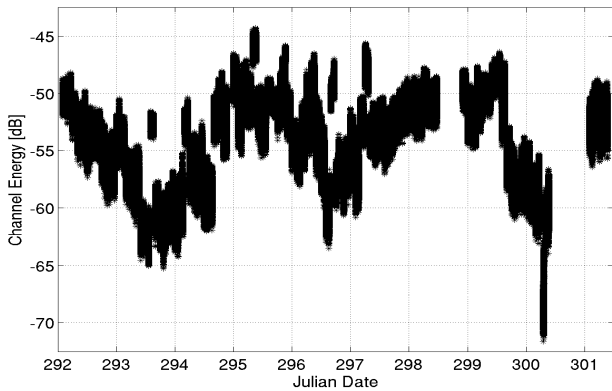


(a) Channel energy time series at S3 from Julian Date 295 to 301.

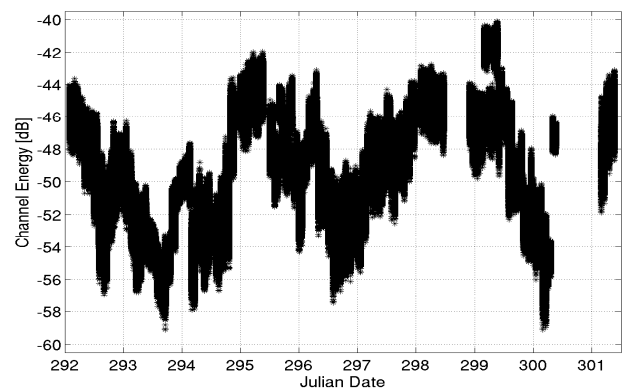


(b) Channel energy time series at S4 from Julian Date 295 to 301.

Fig. 4. Channel energy of the link between the source and receiving stations S3 and S4 (200 m Southeast and Southwest).



(a) Channel energy time series at S5 from Julian Date 295 to 301.



(b) Channel energy time series at S6 from Julian Date 295 to 301.

Fig. 5. Channel energy of the link between the source and receiving stations S5 and S6 (1000 m Southeast and Southwest).

and GS, and for each surrogate data we do the same, i.e., we have J sets with N distances each. We consider the variance of each set of N distances, hence only a value for the original data which we will indicate as Θ_1 and J values for the surrogates, which we will indicate as a vector Θ_0 . The authors in [3] showed that the elements of Θ_0 can be thought as realizations of a random variable γ distributed according to a Gamma distribution, which can be represented by the following probability distribution function:

$$f(x; a, b) = x^{a-1} \frac{\exp(-x/b)}{b^a \Gamma(a)} \text{ for } x \geq 0, \quad (8)$$

where a and b are two positive parameters. Thanks to this result, we can estimate the parameters of the Gamma distribution from the variances computed on surrogates. We choose a probability of failure of the test (in our case 5%) and, from the cumulative distribution function, we determine the threshold of the variance such that the probability that the variance is less than or equal to that threshold is 95% (we will call this threshold α). Then the test can be written as:

$$d(x) = \begin{cases} 1 & \text{if } \Theta_1 > \alpha : \text{non stationary;} \\ 0 & \text{if } \Theta_1 \leq \alpha : \text{stationary.} \end{cases} \quad (9)$$

When the hypothesis of stationarity is rejected, a measure of non-stationarity, which is called index of non-stationarity

(INS) is defined as

$$\text{INS} := \sqrt{\frac{\Theta_1}{E[\gamma]}}, \quad (10)$$

where $E[\gamma]$ is the average value of the random variable, which we approximate as the average of the elements in the vector Θ_0 . Given that the INS depends on the length of the Hermite window T_h , the authors in [3] defined a scale of non-stationarity (SNS) which is the normalized value of T_h such that the INS is maximum:

$$\text{SNS} = \frac{1}{T} \arg \max_{T_h} \text{INS}(T_h). \quad (11)$$

This scale of non-stationarity gives a measure of how variable the process is. In this work we do not compute this measure, because we are primarily interested in the stationarity interval, but leave it as an interesting topic for future study.

B. The Interval of Stationarity

In this subsection we present the results of the stationarity test and the estimate of the interval of stationarity. In particular, we are interested in assessing the wide-sense stationarity over different time scales: a short time scale (of the order of tenths of a second) which concerns physical layer applications, and

a long time scale (of the order of tens of seconds) for upper layer applications, such as Automatic Repeat reQuest (ARQ), medium access control (MAC) and routing protocols. For example, we want to understand whether or not we can assume stationarity in case we want to develop a predictor of the link quality in the second layer of the ISO/OSI architecture, which is responsible for packet reliability and for medium access control. In this case we can trigger decisions, such as not to access the channel in the next step because the predicted channel quality is bad. Nevertheless, for a scenario where the distances of nodes are between some hundreds of meters to a few kilometers, the packet travel time³ is between tenths of seconds to one second⁴, so that, considering the feedback and possible retransmissions allowed in the protocol, the delivery time becomes of the orders of a few seconds.

In the implementation of the procedure [13], we test the stationarity of the process in a time window three minute long, and we choose to compute $J = 50$ randomizations. T_h is varied from 1001 to a third of the length of the time series, with increments of 500 samples at every iteration. We estimate the spectrum by using the first 10 Hermite functions and we estimate the Gamma distribution parameters as maximum-likelihood estimates.

The test, performed on the whole data set, gives as a result that the process is stationary for all the considered T_h . Therefore the process is stationary over at least a three-minute period. This is verified for all the receiving systems. This implies that we can study data adaptive estimators for both the physical and the upper layers, assuming stationarity for the received energy process. Moreover, thanks to this result, we can estimate the PSD of the overall energy over three-minute intervals, in order to see how variable the spectrum is over time. This and some further insights are presented in the following subsection.

C. The PSD of the channel energy

In this subsection we show the PSD estimated over a time interval three minutes long, during which we have tested the stationarity. Specifically, we consider systems in the middle range S3 and S4, at which the intensity of the fluctuations over periods of a few seconds is more evident than at systems S5 and S6, where the acoustic waves are more attenuated. We represent the PSD only for positive frequencies, because the spectrum is a symmetric function, given that the energy time series is a sequence of positive real numbers. Specifically, we want to focus on the intensity of variations of the order of few seconds, therefore we will show the PSD in the range $[0, 1]$ Hz. The PSD is estimated as

$$S(m, f) = \frac{T_s}{N} \left| \sum_{t=1}^N E_g(t) w(t) \exp(-i2\pi ft) \right|^2 \quad (12)$$

³The travel time is the time that the sound wave needs to propagate from the transmitter to the receiver.

⁴We consider here a sound speed of 1500 m/s, and distances between 200 m and 1500 m

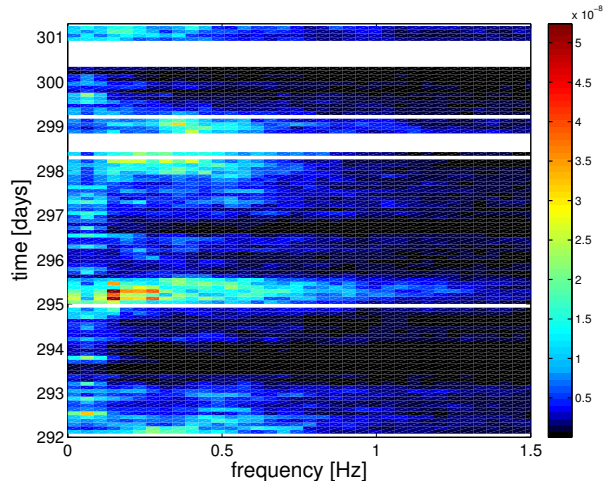


Fig. 6. Pseudocolor plot of the estimated PSD (linear scale) of the channel energy at system S3, from October 18 to 27. The white periods correspond to a lack of measured data.

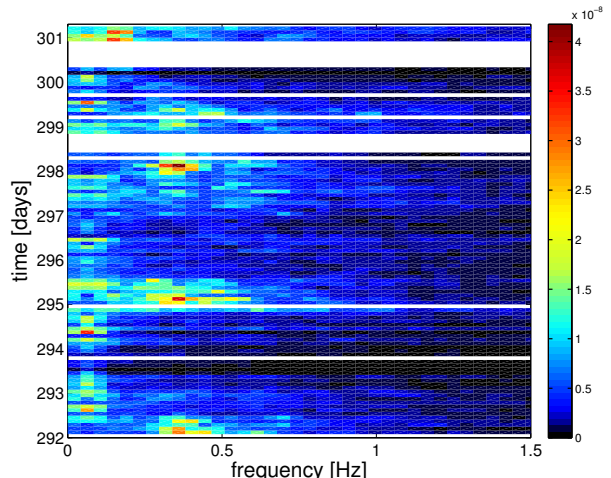


Fig. 7. Pseudocolor plot of the estimated PSD (linear scale) of the channel energy at system S4, from October 18 to 27. The white periods correspond to a lack of measured data.

where $w(t)$ is the Hamming window, $E_g(t)$ is the channel energy process, and m is the index of the epoch of the measurement.

Figures 6 and 7 show the pseudocolor plot of the estimated PSD: frequencies are shown in the x -axis, while Julian dates, at which data were collected, are indicated in the y -axis. We observe that the PSD for system S4 reveals a peak at 0.3 Hz, which corresponds to a three seconds period of the intensity fluctuations of the channel. This is observed at dates 292, 295 and 298. Similar considerations apply also for system S3, although the peaks are less evident.

Figure 8 shows the pseudocolor plot of the magnitude of the impulsive channel response during Julian date 298 at 4 AM for system S4. It can be noticed that the second arrival has almost three peaks every ten seconds, which corresponds

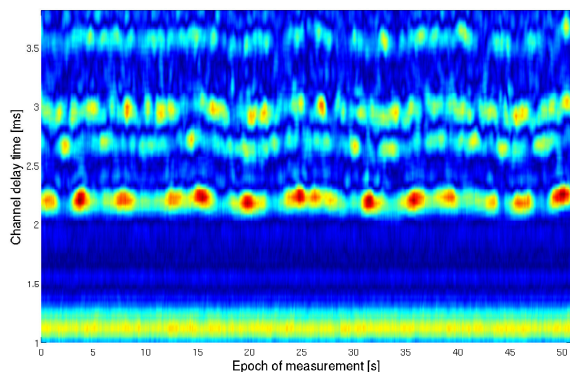


Fig. 8. Pseudocolor plot of the channel impulse response at S4, during Julian date 298.

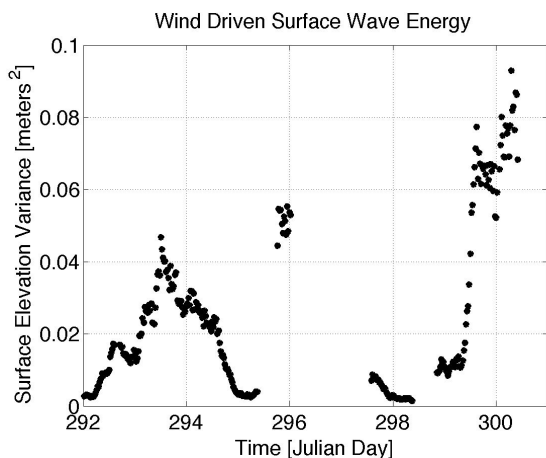


Fig. 9. Time series of the wind driven surface wave energy.

to a peak at frequency 0.3 Hz in the PSD. This behavior can be explained by considering the environmental conditions, and in particular the wind driven wave energy in the surface wave spectra between 0.2 Hz and 0.6 Hz, which is shown in Figure 9.

During the periods of low wind driven waves, as those at dates 292, 295 and 298, the surface wave is coherent over a large spatial region. This results in a greater area of coherent reflection, which is modulated by the regular periodicity of the surface roughness. This area of coherent reflection gives rise to large and periodic fluctuations of the overall energy, such as those observed in Figure 8. On the other hand, when there are higher wind waves, such as those during dates 293, 296 and 300, the coherence of the scattering off the surface is broken, decreasing the area of coherent reflection. This causes many individually fluctuating but smaller intensity arrivals, whose overall energy fluctuations are slower and less intense. From Figures 6 and 7 we can see how variable the spectrum is over long periods of time, which shows that the problem of understanding the stationarity time scale was well-founded even for static underwater channels. This study shows the importance of the hypothesis evaluation, in order to both construct predictors and develop better models for shallow

water propagation.

IV. CONCLUSION AND FUTURE WORK

In this paper we studied the stationarity and evaluated the interval of stationarity of the energy of an underwater acoustic channel. More specifically, we observed that, on average, different links are characterized by at least three minutes long intervals of stationarity. We provided a qualitative explanation of the results by considering the relationship between the environmental fluctuations and the stationarity of the acoustic channel. This work is a first step of a more complete study that we want to perform. Our future work will focus on the extension of this approach to different metrics to represent the channel quality, also including the case of coherent receivers, where phase changes affect the system performance. In addition, a characterization of the cyclo-stationarity of the channel quality will be useful in order to identify and exploit any periodicity of the statistics of the channel in the design of communications and networking protocols.

ACKNOWLEDGMENT

This work has been supported by ONR under Grants no. N00014-05-10085 and N00014-10-10422, by the European Commission under the Seventh Framework Programme (Grant Agreement 258359 – CLAM) and by the Aldo Gini Foundation, Padova, Italy.

REFERENCES

- [1] L. Freitag, M. Grund, S. Singh, J. Partan, P. Koski, and K. Ball, "The WHOI Micro-Modem: An Acoustic Communications and Navigation System for Multiple Platforms," <http://www.whoi.edu>, 2005.
- [2] "Teledyne benthos undersea systems," www.benthos.com.
- [3] P. Borgnat, P. Flandrin, P. Honeine, C. Richard, and J. Xiao, "Testing stationarity with surrogates: A time-frequency approach," *IEEE Transactions on Signal Processing*, vol. 58, no. 7, pp. 3459–3470, Jul. 2010.
- [4] M. B. Priestley and T. S. Rao, "A test for non-stationarity of time-series," *J. of the Royal Statistical Society, Ser. B*, vol. 31, no. 1, pp. 140–149, 1969.
- [5] P. Basu, D. Rudoy, and P. J. Wolfe, "A nonparametric test for stationarity based on local Fourier analysis," in *Proc. of IEEE International Conference on Acoustics, Speech and Signal Processing*, Apr. 2009, pp. 3005–3008.
- [6] M. Herdin, N. Czink, H. Ozcelik, and E. Bonek, "Correlation matrix distance, a meaningful measure for evaluation of non-stationary MIMO channels," in *Proc. of IEEE Vehicular Technology Conference*, May 2005, pp. 136–140.
- [7] T. J. Willink, "Wide-sense stationarity of mobile MIMO radio channels," *IEEE Transactions on Vehicular Technology*, vol. 57, no. 2, pp. 704–714, Mar. 2008.
- [8] D. Umansky and M. Patzold, "Stationarity test for wireless communication channels," in *Proc. of IEEE GLOBECOM*, Dec. 2009, pp. 1–6.
- [9] O. Renaudin, V.-M. Kolmonen, P. Vainikainen, and C. Oestges, "About the multipath stationarity of car-to-car channels in the 5 GHz band," in *Proc. of URSI International Symposium on Electromagnetic Theory (EMTS)*, Aug. 2010, pp. 872–875.
- [10] www.whoi.edu/mvco.
- [11] J. Preisig, "Acoustic propagation considerations for underwater acoustic communications network development," *SIGMOBILE Mob. Comput. Commun. Rev.*, vol. 11, pp. 2–10, Oct. 2007.
- [12] M. Basseville, "Distance measures for signal processing and pattern recognition," *Signal Process.*, vol. 18, pp. 349–369, Dec. 1989.
- [13] P. Borgnat and P. Flandrin and P. Honeine and C. Richard and J. Xiao, http://perso.ens-lyon.fr/pierre.borgnat/codes.html#Stationarity_Tests.